

A Pulsar-Based Map of Galactic Acceleration

Abigail Moran,^{1,*} Chiara M. F. Mingarelli,^{2,1,3} Ken Van Tilburg,^{3,4} and Deborah Good^{1,3}

¹*Department of Physics, University of Connecticut,
196 Auditorium Road, U-3046, Storrs, CT 06269-3046, USA*

²*Department of Physics, Yale University, New Haven, CT 06520, USA*

³*Center for Computational Astrophysics, Flatiron Institute, 162 Fifth Ave, New York, NY 10010, USA*

⁴*Center for Cosmology and Particle Physics, Department of Physics,
New York University, New York, NY 10003, USA*

(Dated: August 15, 2023)

Binary pulsars can be used to probe Galactic potential gradients through calculating their line-of-sight accelerations. We present the first data release of direct line-of-sight acceleration measurements for 28 binary pulsars. We validate these data with a local acceleration model, and compare our results to those extracted from indirect methods. We find evidence for an acceleration gradient in agreement with these values, with our results indicating a local disk density of $\rho_d = 0.036^{+0.020}_{-0.021} \text{ M}_\odot \text{pc}^{-3}$. We also find evidence for unmodeled noise of unknown origin in our data set.

I. INTRODUCTION

Characterizing the distribution of matter in the Milky Way (MW) is crucial for determining the microphysics of dark matter and the dynamical history of our Galaxy. The MW's mass distribution has been partially constrained by its circular rotation curve [1, 2]. These measurements, in conjunction with baryonic mass models, can determine the dark matter distribution [3]. Several analyses [4–7] of velocity-distance data have estimated the midplane density assuming the MW is in dynamic equilibrium, an assumption now known not to hold [8–10].

Stellar velocities from future spectroscopic surveys may serve as a sensitive, direct probe of Galactic acceleration [11–14]. Other model-independent dark matter measurements with transverse angular accelerations [15] are possible using *Gaia* astrometry [16]. Even the fine-grained substructure in the MW may be detectable with pulsar timing arrays (PTAs) [17, 18], and through gravitational lensing of stellar motions [19].

The ultra-stable millisecond pulsars (MSPs) used in PTA experiments are normally used to search for gravitational waves (GWs)[20–23] and to test general relativity [24]. Most of these pulsars have binary companions [25], and secular changes in their orbital periods P_b are measurable for a select few of these. There are also a few several standard binary pulsars which have measured orbital period derivatives.

The change of the binary pulsar's period, \dot{P}_b , has been used to estimate pulsar distances through the Shklovskii effect [26, 27] assuming a fixed Galactic acceleration model. One can also evaluate the predictions of modified gravity theories by studying \dot{P}_b [28], as well as search for GWs with frequencies below 10^{-9} Hz [29, 30]. Recently, there has been interest to use well-timed binary pulsars to directly measure line-of-sight accelerations [31–33]. This

acceleration is a direct probe of the relative gradient of the MW's gravitational potential at the pulsars' locations.

Previously, Ref. [33] reported this acceleration for PSR J1713+0747. Refs. [31, 32] also measured Galactic accelerations using 13 and 14 binary pulsars, respectively. However, Refs. [31, 32] did not directly report individual accelerations nor their associated uncertainties, which we do here for the first time.

Our main result is an open data release of directly measured Galactic accelerations, uncertainties, and other supplementary observables for 28 pulsars. We also perform parameter estimation for the local acceleration gradients and density of the Galactic disk's midplane, and include for the first time a more sophisticated model that includes spurious acceleration noise.

This Letter is laid out as follows: in Sec. II, we describe how to directly infer line-of-sight acceleration from the pulsar data, and a simple model for Galactic acceleration. In Sec. III, we detail our pulsar selection criteria. We benchmark our catalog in Sec. IV with a Markov Chain Monte Carlo (MCMC) analysis to estimate the parameters of this Galactic acceleration model. A summary of our catalog can be found in Table I of the Supplemental Material, and an accompanying .csv file is available with this paper [34].

II. GALACTIC ACCELERATION

The observed time derivative of a binary pulsar's orbit, \dot{P}_b^{Obs} , is a combination of several factors [35]:

$$\dot{P}_b^{\text{Obs}} = \dot{P}_b^{\text{Kin}} + \dot{P}_b^{\text{GW}} + \dot{P}_b^{\text{Gal}} + \dot{P}_b^{\text{n}}, \quad (1)$$

where \dot{P}_b^{Kin} arises from kinematic effects [26], \dot{P}_b^{GW} from GW emission [36], and \dot{P}_b^{Gal} from Galactic acceleration. We introduce \dot{P}_b^{n} , a noise term encapsulating hidden nuisance effects on the binary period due to undetected companions [37–39], accretion, or other unknowns (e.g. baryon loss [40, 41]).

* abigail.moran@uconn.edu

The kinematic term is also called the Shklovskii effect [26]:

$$\dot{P}_b^{\text{Kin}} = \mu^2 r \frac{P_b}{c}, \quad (2)$$

where μ is the proper motion of the pulsar, r is its distance, and c is the speed of light. The GW emission term [42] is:

$$\dot{P}_b^{\text{GW}} = -\frac{192\pi G^{\frac{5}{3}}}{5c^5} F(e) \left(\frac{P_b}{2\pi} \right)^{-\frac{5}{3}} \frac{M_p m_c}{(M_p + m_c)^{\frac{1}{3}}}, \quad (3)$$

where e is the eccentricity of the binary orbit, $F(e) = (1 - e^2)^{-\frac{7}{2}} (1 + \frac{73e^2}{24} + \frac{37e^4}{96})$ which is unity for circular orbits, and M_p and m_c are the masses of the pulsar and companion, respectively. When the pulsar's mass is not known, we approximate $M_p = 1.57 \pm 0.35 M_\odot$, which is the average mass of a millisecond pulsar [43], and m_c is constrained for every pulsar system which meets our other criteria. When eccentricities are unknown, we approximate $e = 0$, since these binaries typically have $e \approx 0$.

We can compute \dot{P}_b^{Gal} by subtracting the kinematic and GW terms from \dot{P}_b^{Obs} and marginalizing over the noise contribution \dot{P}_b^{n} in Eq. 1. We can furthermore write the differential Galactic line-of-sight acceleration as

$$\mathbf{a}_{\text{Gal}} \cdot \hat{\mathbf{r}} = c \frac{\dot{P}_b^{\text{Gal}}}{P_b} = - \left[\nabla \Phi(\mathbf{r}_b) - \nabla \Phi(\mathbf{r}_\odot) \right] \cdot \hat{\mathbf{r}}, \quad (4)$$

where $\hat{\mathbf{r}} \equiv \mathbf{r}/|\mathbf{r}|$, the distance to the pulsar is $\mathbf{r} = \mathbf{r}_b - \mathbf{r}_\odot$, and Φ is the gravitational potential. The difference in gradient of the gravitational potential between the Earth (\mathbf{r}_\odot) and the binary pulsar (\mathbf{r}_b) can be directly measured with P_b and \dot{P}_b^{Gal} .

We estimate the parameters of the following model for the Galactic acceleration:

$$\mathbf{a}_{\text{Gal}}(\mathbf{r}) = a'_x \hat{\mathbf{x}} (\hat{\mathbf{x}} \cdot \mathbf{r}) + a'_z \hat{\mathbf{z}} (\hat{\mathbf{z}} \cdot \mathbf{r}), \quad (5)$$

where $\hat{\mathbf{x}}$ and $\hat{\mathbf{z}}$ are unit vectors in galactocentric coordinates, pointing away from the Galactic Center and towards the Galactic North Pole (perpendicular to the disk), respectively. The fit parameters in Eq. 5 are the Taylor expansion coefficients of the local acceleration field, with a'_x directly related to the slope of the MW's rotation curve, and the vertical acceleration gradient a'_z (primarily) to the density of the Galactic disk ρ_d through Poisson's equation:

$$a'_z \simeq 4\pi G \rho_d. \quad (6)$$

This local expansion should be a good approximation since the pulsars in our sample populate the local Galactic neighborhood and are predominantly inside the galactic disk (more in Sec. III).

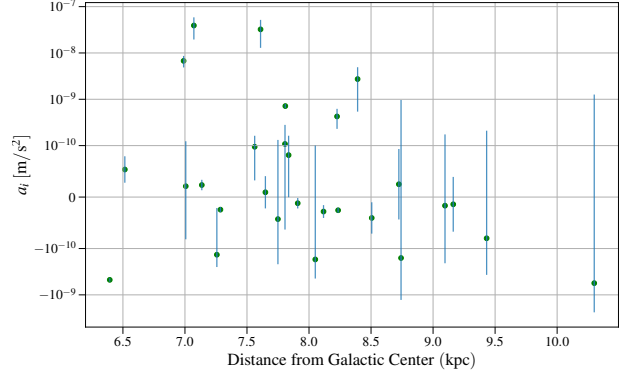


FIG. 1. Line-of-sight acceleration of each binary pulsar as a function of distance from the Galactic Center. Error bars include uncertainties propagated from measurements of proper motion, distance, and timing parameters only, and do not include the additional acceleration noise parameter, \dot{P}_b^{n} .

III. PULSAR CATALOG CONSTRUCTION

We search the Australia Telescope National Facility's (ATNF) pulsar catalog [44] for all pulsars with P_b and \dot{P}_b^{Obs} measurements. We select pulsars with measured proper motion, and distance based on astrometric parallax or timing parallax, necessary to calculate the Shklovskii effect in Eq. 2. If a pulsar is missing a parallax measurement, we obtain the distance to the companion (and thus the binary) using techniques from Refs. [45, 59]. We use this technique to update the distance to J0348+0432 to 1594^{+1178}_{-619} pc [59].

We exclude pulsars in globular clusters since these have accelerations that are not expected to conform to our simple model in Eq. 5. We further exclude pulsars in the accretion stage of evolution and “spider pulsars”. These are accreting from their companions, which can cause the binary period to decrease [46]. This selection returns 28 pulsars, see Supplemental Material's Figs. 1 and 4 [34] for their distribution in the Galactic plane.

IV. RESULTS

We directly compute the line-of-sight acceleration for the 28 pulsars in our catalog—the largest of its kind. We deduce each pulsar's acceleration from the data as

$$a_i = c P_{b,i}^{-1} \left[\dot{P}_{b,i}^{\text{Obs}} - \dot{P}_{b,i}^{\text{Kin}} - \dot{P}_{b,i}^{\text{GW}} \right], \quad (7)$$

via Eq. 1 and the first equality in Eq. 4. The observational uncertainties on a_i , denoted by $\sigma_{a,i}$, are the quadrature sums of the uncertainties for each of the terms in Eq. 7. In Fig. 1, we show a_i and $\sigma_{a,i}$ as a function of distance from the Galactic Center. Fig. 2 and Fig. 3 of the Supplemental Material show maps of these data [34].

To assess the quality and sensitivity of our pulsar acceleration catalog, we perform an MCMC analysis of the pa-

rameters of the simple local acceleration model of Eq. 5. We find that the sum of kinematic, GW, and Galactic acceleration contributions does not adequately explain the data: a small (but larger than expected) subset of binary period derivatives are outliers in the fits for any physically reasonable Galactic acceleration model (several standard deviations from the best fit predictions of Eq. 5).

We postulate that, with a probability p_n , any binary pulsar is subject to an additional, unknown acceleration noise $\mathbf{a}_n = a_n \hat{\mathbf{R}}_n$ as a nuisance parameter in a random direction $\hat{\mathbf{R}}_n$. The probability density function (PDF) for the angle $\theta_n \equiv \arccos(\hat{\mathbf{a}}_n \cdot \hat{\mathbf{r}}_i)$, where $0 \leq \theta_n \leq \pi$, is thus $\sin(\theta_n)/2$. The magnitude of the acceleration is taken to have the normalized PDF $C a_n^{-\zeta}$ with normalization coefficient $C = (\zeta - 1)/[(a_n^{\min})^{-\zeta+1} - (a_n^{\max})^{-\zeta+1}]$. The minimum noise acceleration is $a_n^{\min} \approx 1.77 \times 10^{-12} \text{ m s}^{-2}$ (less than the smallest inferred acceleration error), corresponding to the constant acceleration from a gravitational perturber of mass $1 M_\oplus$ and semimajor axis 100 AU in a circumbinary orbit. The maximum noise acceleration is $a_n^{\max} = 2.94 \times 10^{-6} \text{ m s}^{-2}$, corresponding to a third body with $0.2 M_\odot$ mass and 20 AU semimajor axis. We are not claiming to have detected triple systems, but this is a physical and plausible example of a model which can generate additional acceleration noise.

The addition of this nuisance acceleration term \mathbf{a}_n leads to the following likelihood function \mathcal{L} for the observed acceleration:

$$\begin{aligned} \mathcal{L}(\{a_i\} | a'_x, a'_z, p_n, \zeta) &= \int_0^\pi d\theta_n \frac{\sin \theta_n}{2} \int_{a_n^{\min}}^{a_n^{\max}} da_n C a_n^{-\zeta} \\ &\prod_{i=1}^N \left[(1 - p_n) f(\Delta a_i, \sigma_{a,i}) + p_n f(\Delta a_i - a_n \cos \theta_n, \sigma_{a,i}) \right]. \end{aligned} \quad (8)$$

The likelihood function takes as input the line-of-sight acceleration estimates $\{a_i\}$ for each pulsar $i = 1, \dots, N$. The function $f(a, \sigma)$ is a normal distribution in a with standard deviation σ . In Eq. 8, we have abbreviated $\Delta a_i \equiv a_i - a_{\text{Gal},i}$ and $a_{\text{Gal},i} \equiv \mathbf{a}_{\text{Gal}}(\mathbf{r}_i) \cdot \hat{\mathbf{r}}_i$ from Eq. 5 defined in terms of a'_x and a'_z .

We assume there is a probability p_n that accretion or other acceleration (from e.g. a third body) is contributing to each pulsar's acceleration a_i . The data in Fig. 1 indicate that there are several large outliers for which this could be the case. Under the assumption of Gaussian errors, these pulsars skew the fit parameters of Eq. 5 as well as any goodness of fit calculations. By introducing p_n and ζ we produce a model which accounts for nuisance acceleration measurements without removing apparent outliers. This modified distribution better reflects the spread in the acceleration data, due to its heavier tail than that of a Gaussian distribution (see e.g. Fig. 2).

In Fig. 2, we plot the resulting likelihood function \mathcal{L} for a *single* pulsar with uncertainty $\sigma_a = 10^{-11} \text{ m/s}^2$ as a function of $|a_i - a_{\text{Gal},i}|$. In the limit of $p_n \rightarrow 0$ or $\zeta \rightarrow \infty$, it reduces to a normal distribution. For non-zero p_n and finite ζ , the distribution has fatter tails with

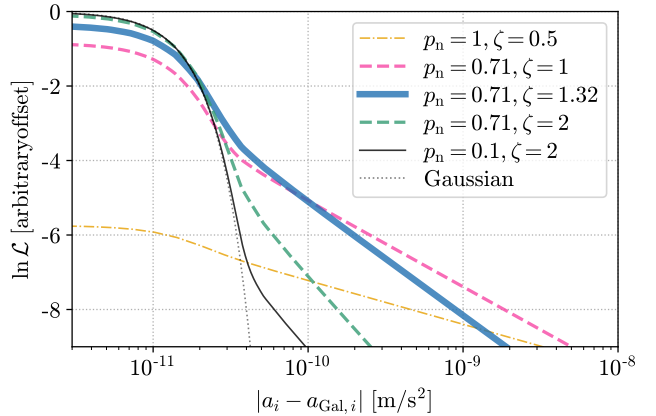


FIG. 2. Log likelihood $\ln \mathcal{L}$ from Eq. 8 (with a fixed global offset) for a single pulsar with (observational) acceleration uncertainty of $\sigma_{a,i} = 10^{-11} \text{ m/s}^2$, as function of $|a_i - a_{\text{Gal},i}|$, the difference from the acceleration model prediction. The blue curve represents the best-fit model from Fig. 3, which is essentially a Gaussian likelihood for small acceleration deviations, but one with fatter tails whose height and slope are controlled by the nuisance parameters p_n (the probability of additional noise) and ζ (the spectral index). We also plot the log likelihoods for other reference values of p_n and ζ , as well as that of a Gaussian distribution (dotted curve).

height proportional to p_n and logarithmic slope controlled by ζ . As long as $\zeta > 1$, the variance of the distribution is essentially independent from the choice of a_n^{\max} , and will not dramatically alter the typical posterior widths (only the tails).

In Fig. 3, we show the posteriors on these four parameters, which are all detected at moderate to high significance. The MCMC analysis assumes flat priors on all parameters a'_x , a'_z , p_n , and ζ , with $0 < p_n < 1$ and $0 < \zeta < 2$. The null hypothesis with $a'_x = a'_z = 0$ is excluded at 2.2σ and 1.8σ significance respectively, and as expected we find that $a'_x > 0$ and $a'_z < 0$. We also find $\zeta = 1.39^{+0.12}_{-0.10}$; such a strong preference for the nuisance acceleration spectral index (and large p_n) indicates the existence of additional noise in the data. The best-fit

Parameter	a'_x	a'_z	ρ_d
Units	$10^{-10} \frac{\text{m}}{\text{s}^2 \text{kpc}}$	$10^{-10} \frac{\text{m}}{\text{s}^2 \text{kpc}}$	$10^{-2} \frac{M_\odot}{\text{pc}^3}$
This Work	$0.30^{+0.12}_{-0.13}$	$-0.63^{+0.36}_{-0.36}$	$3.6^{+2.0}_{-2.1}$
Ref. [47]	$0.16^{+0.54}_{-0.50}$	$-0.98^{+0.54}_{-0.55}$	$5.6^{+3.1}_{-3.1}$
Ref. [5]	—	$-1.78^{+0.18}_{-0.18}$	$10.2^{+1.0}_{-1.0}$
Ref. [48]	—	$-1.3^{+0.3}_{-0.3}$	$7.6^{+1.5}_{-1.5}$
Ref. [32]	—	$-1.52^{+0.83}_{-0.37}$	8^{+5}_{-2}

TABLE I. Best-fit parameters for the Galactic acceleration gradients a'_x and a'_z in the radial and vertical directions (cfr. Eq. 5), respectively, and corresponding density ρ_d in the midplane of the MW disk via Eq. 6.

values $\zeta = 1.39$ and $p_n = 0.71$ from Fig. 3 are shown in Fig. 2. Note that the preferred spectral index is significantly larger than unity. In addition, the noise probability is pushing up close to the physically sensible boundary of $p_n = 1$, but since a_n^{\min} is so small, this effectively still corresponds to a small probability of *significant* excess noise for all pulsars. Future timing data may identify its physical origin, e.g. accretion in these binary systems.

We summarize the results for the radial and vertical acceleration gradients and the corresponding midplane Galactic disk density (via Eq. 6) in Tab. I. We compare them to the corresponding parameters estimated in Ref. [47] using the orbital arc method [49], and in Refs. [5, 48] using Jeans analyses methods based on *Hipparcos* data. The latter analyses need to assume dynamical equilibrium in the MW, and arrive at values somewhat higher than ours for the disk density, though within 3.3 and 2.0σ of our results, respectively. Ref. [32] similarly uses binary pulsars to estimate the parameters of a local acceleration model, but does not include a nuisance parameter, and includes an a'_ϕ term. Our vertical acceleration gradient measurement is 1.04σ from what they find and the derived densities differ by 2.2σ .

We introduce a modified chi-squared distribution ($\tilde{\chi}^2$) to evaluate the model's goodness of fit:

$$\tilde{\chi}^2 = 2 \left(\text{erfc}^{-1} [2(1 - \mathcal{L}(\delta a_i, \sigma_{a,i}, p_n, \zeta))] \right), \quad (9)$$

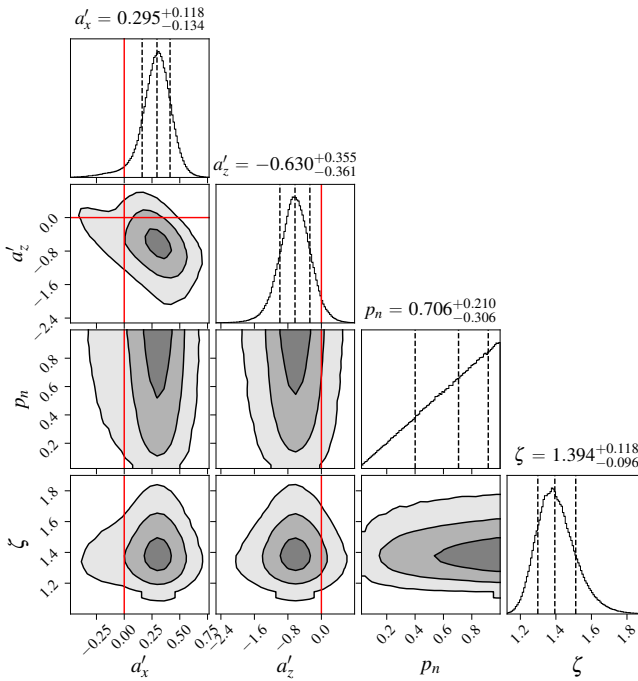


FIG. 3. Posterior distributions for galactic acceleration gradients in the radial (a'_x) and vertical (a'_z) directions (see Eq. 5), the probability (p_n) that a pulsar has an additional acceleration in a random direction, and the spectral index (ζ) for the magnitude of this additional acceleration noise. The acceleration gradients are quoted in units of $[10^{-10} \text{ m/s}^2/\text{kpc}]$. Red vertical and horizontal lines indicate $a'_x = a'_z = 0$, and dashed black lines delineate the 16th, 50th, and 84th percentiles.

where erfc^{-1} is the inverse complementary error function. This modified distribution is constructed such that $\tilde{\chi}^2 = n^2$ has the same p -value under the likelihood of Eq. 8 for finite p_n and ζ (see Fig. 2) as $\chi^2 = n^2$ (an n -sigma deviation) for the standard chi-square distribution under a Gaussian likelihood. In particular, Eq. 9 approaches the standard χ^2 value in the limit $p_n \rightarrow 0$ or $\zeta \rightarrow \infty$. In Tab. II, we show measurements of goodness of fit for the null hypothesis ($a_{\text{Gal}} \equiv 0$) and Eq. 5 using the best fit parameters shown in Table I. We find that Eq. 5 is a better fit to the acceleration data, both when assuming Gaussian errors (χ^2) and when using the modified distribution $\tilde{\chi}^2$, which effectively always yields a good fit by construction.

The results from Tab. II strongly suggest the presence of additional noise sources which have previously not been taken into account. We handle this excess noise with two nuisance parameters (p_n and ζ), and show that the direct evidence for acceleration gradients previously suggested in Refs. [31–33] survives under this more robust model. Our more sophisticated, non-Gaussian errors establish statistical concordance with the data, as evidenced by the last column of Tab. II. The physical origin of this excess acceleration noise is unknown, and should be explored in future work.

V. DISCUSSION

We present a direct map of Galactic acceleration measurements based on a comprehensive catalog constructed from ATNF and *Gaia* data. These data can be fit to models of the Galactic potential or matter density [32]. Our analysis constrains the Galactic midplane density to $0.036^{+0.020}_{-0.021} M_\odot \text{ pc}^{-3}$ which is within 2σ of results from Refs. [47, 48]. Our 28 data points with 4 fit parameters, reported in Table II, “match” the model of Galactic acceleration given in Eq. 5 with a high Gaussian chi-square value of $\chi^2 = 1390$. Refs. [31, 32] use a similar Gaussian-based method to report their accelerations. We find six outlier ($\gtrsim 2\sigma$) acceleration measurements: those from PSRs B1913+16 (34.5σ), J0437-4715 (4.3σ), J1713+0747 (6.4σ), J1741+1351 (3.6σ), J2129-5721 (10.3σ), and J2339-0533 (2.5σ). PSR J2239-0533 is outside the disk, with $z = -1256$ pc, and therefore may have a_i mismodeled by Eq. 5 by order one in the z -direction. Two of the remaining outliers, B1913+16 and

Model	χ^2	$\tilde{\chi}^2$
No acceleration (null)	1174	39.29
Galactic acceleration (Eq. 5)	1390	35.77

TABLE II. Goodness of fit for the null hypothesis ($a_{\text{Gal},i} = 0$) and the Galactic acceleration model of Eq. 5. We report the standard χ^2 values, as well as a modified statistic $\tilde{\chi}^2$ from Eq. 9 based on the likelihood from Eq. 8.

J0437-4715 are located well inside the galactic disk, so we expect Eq. 5 to be a valid model for these accelerations. PSRs J1713+0747, J1741+1351, and J2129-5721 are outside of the thin galactic disk, but inside the thick disk. The expansion from Eq. 5 thus mildly overestimates the acceleration magnitude, but this mismodeling is not nearly enough to account for the large discrepancies. Given that the outliers cannot be accommodated by any plausible galactic acceleration model, we reject the Gaussian noise hypothesis, and explore the possibility of an additional spurious noise term contributing to \dot{P}_b^{Obs} .

We model this with the nuisance parameter \mathbf{a}_n in Eq. 9. We find a significant improvement in the subsequent modified $\tilde{\chi}^2 \approx 36$ (see Tab. II) and tight constraints on ζ (see Tab. I). This indeed indicates that several of the outliers discussed above are the result of data quality issues (though we eliminated known systematic effects), intrinsic physical processes such as undetected accretion in the pulsar binary, or rare occurrences of significant acceleration caused by a third body in a wide circumbinary orbit [50].

Assuming the modified likelihood function given by Eq. 8, PSR J1741+1351 is the only significant ($> 2\sigma$) outlier. The acceleration, a_i , derived from J1741+1351 differs from the prediction of the best-fit model of Eq. 5 by 2.4σ , down from 3.6σ using Gaussian noise. The distance to this pulsar is derived from nearly a decade of timing data [51]. The orbital parameters to the pulsar have also been updated using [52], making it unlikely that any parameters are grossly mischaracterized. We are thus confident in our inferred a_i .

The error associated with P_b improves as $T^{-3/2}$ with integration time T , so \dot{P}_b^{Obs} improves as $T^{-5/2}$ [53]. Par-

allax errors, used in the computation of \dot{P}_b^{Kin} , also improve as $T^{-1/2}$ [54], and are expected to improve by $(66 \text{ months}/34 \text{ months})^{-1/2} \sim 0.7$ in *Gaia* DR4. Of the 28 pulsar acceleration measurements in our catalog, 18 are limited by \dot{P}_b^{Obs} errors, and 9 are dominated by uncertainties on the \dot{P}_b^{Kin} determination (primarily parallax error), and 1 is limited by P_b^{GW} . We are therefore hopeful that our few-sigma measurement of acceleration gradients will turn into a precision probe of Galactic structure with future pulsar timing data releases and correspondingly improved line-of-sight acceleration catalogs.

ACKNOWLEDGMENTS

We thank Sukanya Chakrabarti, William DeRocco, Susan Gardner, Matthew Kerr, Mariangela Lisanti, Katelin Schutz, and Oren Slone for helpful conversations and feedback. The Center for Computational Astrophysics is a division of the Flatiron Institute in New York City, which is supported by the Simons Foundation. This research was supported in part by the National Science Foundation under Grants No. NSF PHY-1748958, PHY-2020265, AST-2106552, and PHY-2210551 and by the NASA CT Space Grant Consortium under P-1935, Undergraduate Research Grant. This work has made use of data from the European Space Agency (ESA) mission Gaia (<https://www.cosmos.esa.int/gaia>), processed by the Gaia Data Processing and Analysis Consortium (DPAC, <https://www.cosmos.esa.int/web/gaia/dpac/consortium>). Funding for the DPAC has been provided by national institutions, in particular the institutions participating in the Gaia Multilateral Agreement.

-
- [1] A.-C. Eilers, D. W. Hogg, H.-W. Rix, and M. K. Ness, The Circular Velocity Curve of the Milky Way from 5 to 25 kpc, *Astrophys. J.* **871**, 120 (2019), arXiv:1810.09466 [astro-ph.GA].
 - [2] M. Benito, F. Iocco, and A. Cuoco, Uncertainties in the Galactic Dark Matter distribution: An update, *Physics of the Dark Universe* **32**, 100826 (2021), arXiv:2009.13523 [astro-ph.GA].
 - [3] E. Pouliasis, P. Di Matteo, and M. Haywood, A Milky Way with a massive, centrally concentrated thick disc: new Galactic mass models for orbit computations, *A&A* **598**, A66 (2017), arXiv:1611.07979 [astro-ph.GA].
 - [4] K. Kuijken and G. Gilmore, The mass distribution in the galactic disc -II. Determination of the surface mass density of the galactic disc near the Sun., *MNRAS* **239**, 605 (1989).
 - [5] J. Holmberg and C. Flynn, The local density of matter mapped by Hipparcos, *MNRAS* **313**, 209 (2000), arXiv:astro-ph/9812404 [astro-ph].
 - [6] J. Bovy and S. Tremaine, On the Local Dark Matter Density, *Astrophys. J.* **756**, 89 (2012), arXiv:1205.4033 [astro-ph.GA].
 - [7] A. Widmark, Measuring the local matter density using *Gaia* DR2, *A&A* **623**, A30 (2019), arXiv:1811.07911 [astro-ph.GA].
 - [8] M. Bennett and J. Bovy, Vertical waves in the solar neighbourhood in *Gaia* DR2, *MNRAS* **482**, 1417 (2019), arXiv:1809.03507 [astro-ph.GA].
 - [9] T. Antoja, A. Helmi, M. Romero-Gómez, D. Katz, C. Babusiaux, R. Drimmel, D. W. Evans, F. Figueras, E. Poggio, C. Reylé, A. C. Robin, G. Seabroke, and C. Soubiran, A dynamically young and perturbed Milky Way disk, *Nature (London)* **561**, 360 (2018), arXiv:1804.10196 [astro-ph.GA].
 - [10] A. P. Naik, J. An, C. Burrage, and N. W. Evans, Charting galactic accelerations - II. How to ‘learn’ accelerations in the solar neighbourhood, *MNRAS* **511**, 1609 (2022), arXiv:2112.07657 [astro-ph.GA].
 - [11] C. Quercellini, L. Amendola, and A. Balbi, Mapping the galactic gravitational potential with peculiar acceleration, *MNRAS* **391**, 1308 (2008), arXiv:0807.3237 [astro-ph].
 - [12] H. Silverwood and R. Easther, Stellar accelerations and the galactic gravitational field, *PASA* **36**, e038 (2019), arXiv:1812.07581 [astro-ph.GA].

- [13] S. Chakrabarti, J. Wright, P. Chang, A. Quillen, P. Craig, J. Territo, E. D’Onghia, K. V. Johnston, R. J. De Rosa, D. Huber, K. L. Rhode, and E. Nielsen, Toward a Direct Measure of the Galactic Acceleration, *ApJL* **902**, L28 (2020), arXiv:2007.15097 [astro-ph.GA].
- [14] A. Ravi, N. Langellier, D. F. Phillips, M. Buschmann, B. R. Safdi, and R. L. Walsworth, Probing Dark Matter Using Precision Measurements of Stellar Accelerations, *Phys. Rev. Lett.* **123**, 091101 (2019), arXiv:1812.07578 [astro-ph.GA].
- [15] M. Buschmann, B. R. Safdi, and K. Schutz, Galactic Potential and Dark Matter Density from Angular Stellar Accelerations, *Phys. Rev. Lett.* **127**, 241104 (2021), arXiv:2103.05000 [astro-ph.GA].
- [16] Gaia Collaboration, A. G. A. Brown, A. Vallenari, T. Prusti, J. H. J. de Bruijne, C. Babusiaux, M. Biermann, O. L. Cleeve, D. W. Evans, L. Eyer, A. Hutton, F. Jansen, C. Jordi, S. A. Klioner, U. Lammers, L. Lindegren, X. Luri, F. Mignard, C. Panem, D. Pourbaix, S. Randich, P. Sartoretti, C. Soubiran, N. A. Walton, F. Arenou, C. A. L. Bailer-Jones, U. Bastian, M. Cropper, R. Drimmel, D. Katz, M. G. Lattanzi, F. van Leeuwen, J. Bakker, C. Cacciari, J. Castañeda, F. De Angeli, C. Ducourant, C. Fabricius, M. Fouesneau, Y. Frémat, R. Guerra, *et al.*, Gaia Early Data Release 3. Summary of the contents and survey properties (Corrigendum), *A&A* **650**, C3 (2021).
- [17] J. A. Dror, H. Ramani, T. Trickle, and K. M. Zurek, Pulsar timing probes of primordial black holes and subhalos, *Phys. Rev. D* **100**, 023003 (2019), arXiv:1901.04490 [astro-ph.CO].
- [18] H. Ramani, T. Trickle, and K. M. Zurek, Observability of dark matter substructure with pulsar timing correlations, *Journal of Cosmology and Astroparticle Physics* **2020** (12), 033, arXiv:2005.03030 [astro-ph.CO].
- [19] K. Van Tilburg, A.-M. Taki, and N. Weiner, Halometry from astrometry, *Journal of Cosmology and Astroparticle Physics* **2018** (7), 041, arXiv:1804.01991 [astro-ph.CO].
- [20] M. V. Sazhin, Opportunities for detecting ultralong gravitational waves, *Soviet Astronomy* **22**, 36 (1978).
- [21] S. Detweiler, Pulsar timing measurements and the search for gravitational waves, *Astrophys. J.* **234**, 1100 (1979).
- [22] R. W. Hellings and G. S. Downs, Upper limits on the isotropic gravitational radiation background from pulsar timing analysis., *ApJL* **265**, L39 (1983).
- [23] C. M. F. Mingarelli and J. A. Casey-Clyde, Seeing the gravitational wave universe, *Science* **378**, 592 (2022), arXiv:2211.05148 [gr-qc].
- [24] K. Lazaridis, N. Wex, A. Jessner, M. Kramer, B. W. Stappers, G. H. Janssen, G. Desvignes, M. B. Purver, I. Cognard, G. Theureau, A. G. Lyne, C. A. Jordan, and J. A. Zensus, Generic tests of the existence of the gravitational dipole radiation and the variation of the gravitational constant, *MNRAS* **400**, 805 (2009), arXiv:0908.0285 [astro-ph.GA].
- [25] D. R. Lorimer, Binary and Millisecond Pulsars, *Living Reviews in Relativity* **8**, 7 (2005), arXiv:astro-ph/0511258 [astro-ph].
- [26] I. S. Shklovskii, Possible Causes of the Secular Increase in Pulsar Periods., *Soviet Astronomy* **13**, 562 (1970).
- [27] J. P. W. Verbiest, M. Bailes, W. van Straten, G. B. Hobbs, R. T. Edwards, R. N. Manchester, N. D. R. Bhat, J. M. Sarkissian, B. A. Jacoby, and S. R. Kulkarni, Precision Timing of PSR J0437-4715: An Accurate Pulsar Distance, a High Pulsar Mass, and a Limit on the Variation of Newton’s Gravitational Constant, *Astrophys. J.* **679**, 675 (2008), arXiv:0801.2589 [astro-ph].
- [28] H. Ding, A. T. Deller, B. W. Stappers, T. J. W. Lazio, D. Kaplan, S. Chatterjee, W. Brisken, J. Cordes, P. C. C. Freire, E. Fonseca, I. Stairs, L. Guillemot, A. Lyne, I. Cognard, D. J. Reardon, and G. Theureau, The MSPSR π catalogue: VLBA astrometry of 18 millisecond pulsars, *MNRAS* **519**, 4982 (2023), arXiv:2212.06351 [astro-ph.HE].
- [29] W. DeRocco and J. A. Dror, Using Pulsar Parameter Drifts to Detect Sub-Nanohertz Gravitational Waves, *arXiv e-prints* , arXiv:2212.09751 (2022), arXiv:2212.09751 [astro-ph.HE].
- [30] W. DeRocco and J. A. Dror, Searching For Stochastic Gravitational Waves Below a Nanohertz, *arXiv e-prints* , arXiv:2304.13042 (2023), arXiv:2304.13042 [astro-ph.HE].
- [31] D. F. Phillips, A. Ravi, R. Ebadi, and R. L. Walsworth, Milky Way Accelerometry via Millisecond Pulsar Timing, *Phys. Rev. Lett.* **126**, 141103 (2021), arXiv:2008.13052 [astro-ph.GA].
- [32] S. Chakrabarti, P. Chang, M. T. Lam, S. J. Vigeland, and A. C. Quillen, A Measurement of the Galactic Plane Mass Density from Binary Pulsar Accelerations, *ApJL* **907**, L26 (2021), arXiv:2010.04018 [astro-ph.GA].
- [33] K. Hefflin and R. Lieu, Galactic orbital effects on pulsar timing, *MNRAS* **504**, 166 (2021), arXiv:2103.15314 [astro-ph.GA].
- [34] See the Supplemental Material at [URL will be inserted by publisher] for a complete catalog of the pulsar and acceleration data.
- [35] J. F. Bell and M. Bailes, New Method for Obtaining Binary Pulsar Distances and Its Implications for Tests of General Relativity, *ApJL* **456**, L33 (1996), arXiv:astro-ph/9510060 [astro-ph].
- [36] J. M. Weisberg and Y. Huang, Relativistic Measurements from Timing the Binary Pulsar PSR B1913+16, *Astrophys. J.* **829**, 55 (2016), arXiv:1606.02744 [astro-ph.HE].
- [37] I. C. Nițu, M. J. Keith, B. W. Stappers, A. G. Lyne, and M. B. Mickaliger, A search for planetary companions around 800 pulsars from the Jodrell Bank pulsar timing programme, *MNRAS* **512**, 2446 (2022), arXiv:2203.01136 [astro-ph.EP].
- [38] R. G. Martin, M. Livio, and D. Palaniswamy, Why are Pulsar Planets Rare?, *ApJ* **832**, 122 (2016), arXiv:1609.06409 [astro-ph.EP].
- [39] M. L. Jones, D. L. Kaplan, M. A. McLaughlin, and D. R. Lorimer, Constraints on Undetected Long-Period Binaries in the Known Pulsar Population, *arXiv e-prints* , arXiv:2305.03561 (2023), arXiv:2305.03561 [astro-ph.HE].
- [40] J. M. Berryman, S. Gardner, and M. Zakeri, How Macroscopic Limits on Neutron Star Baryon Loss Yield Microscopic Limits on Non-Standard-Model Baryon Decay, *arXiv e-prints* , arXiv:2305.13377 (2023), arXiv:2305.13377 [hep-ph].
- [41] J. M. Berryman, S. Gardner, and M. Zakeri, Neutron Stars with Baryon Number Violation, Probing Dark Sectors, *Symmetry* **14**, 518 (2022), arXiv:2201.02637 [hep-ph].
- [42] I. I. Shapiro, Fourth Test of General Relativity, *Phys. Rev. Lett.* **13**, 789 (1964).

- [43] C. M. Zhang, J. Wang, Y. H. Zhao, H. X. Yin, L. M. Song, D. P. Menezes, D. T. Wickramasinghe, L. Ferrario, and P. Chardonnet, Study of measured pulsar masses and their possible conclusions, *A&A* **527**, A83 (2011), arXiv:1010.5429 [astro-ph.HE].
- [44] R. N. Manchester, G. B. Hobbs, A. Teoh, and M. Hobbs, The Australia Telescope National Facility Pulsar Catalogue, *AJ* **129**, 1993 (2005), arXiv:astro-ph/0412641 [astro-ph].
- [45] C. M. F. Mingarelli, L. Anderson, M. Bedell, D. N. Spergel, and A. Moran, Improving Binary Millisecond Pulsar Distances with Gaia, arXiv e-prints , arXiv:1812.06262 (2018), arXiv:1812.06262 [astro-ph.IM].
- [46] L. A. Rawley, J. H. Taylor, and M. M. Davis, Period derivative and orbital eccentricity of binary pulsar 1953+29, *Nature (London)* **319**, 383 (1986).
- [47] R. Kipper, P. Tenjes, E. Tempel, and R. de Propris, Non-equilibrium in the solar neighbourhood using dynamical modelling with Gaia DR2, *MNRAS* **506**, 5559 (2021), arXiv:2106.07076 [astro-ph.GA].
- [48] M. Creze, E. Chereul, O. Bienayme, and C. Pichon, The distribution of nearby stars in phase space mapped by Hipparcos. I. The potential well and local dynamical mass, *A&A* **329**, 920 (1998), arXiv:astro-ph/9709022 [astro-ph].
- [49] R. Kipper, E. Tempel, and P. Tenjes, A method to calculate gravitational accelerations within discrete localized regions in the Milky Way, *MNRAS* **482**, 1724 (2019), arXiv:1809.06616 [astro-ph.GA].
- [50] S. M. Ransom, I. H. Stairs, A. M. Archibald, J. W. T. Hessels, D. L. Kaplan, M. H. van Kerkwijk, J. Boyles, A. T. Deller, S. Chatterjee, A. Schechtman-Rook, A. Berndsen, R. S. Lynch, D. R. Lorimer, C. Karakoc-Argaman, V. M. Kaspi, V. I. Kondratiev, M. A. McLaughlin, J. van Leeuwen, R. Rosen, M. S. E. Roberts, and K. Stovall, A millisecond pulsar in a stellar triple system, *Nature (London)* **505**, 520 (2014), arXiv:1401.0535 [astro-ph.SR].
- [51] Z. Arzoumanian, A. Brazier, S. Burke-Spolaor, S. Chamberlin, S. Chatterjee, B. Christy, J. M. Cordes, N. J. Cornish, F. Crawford, H. Thankful Cromartie, K. Crowter, M. E. DeCesar, P. B. Demorest, T. Dolch, J. A. Ellis, R. D. Ferdman, E. C. Ferrara, E. Fonseca, N. Garver-Daniels, P. A. Gentile, D. Halmrast, E. A. Huerta, F. A. Jenet, and NANOGrav Collaboration, The NANOGrav 11-year Data Set: High-precision Timing of 45 Millisecond Pulsars, *ApJS* **235**, 37 (2018), arXiv:1801.01837 [astro-ph.HE].
- [52] G. Agazie, M. F. Alam, A. Anumarlapudi, A. M. Archibald, Z. Arzoumanian, P. T. Baker, L. Blecha, V. Bonidie, A. Brazier, P. R. Brook, S. Burke-Spolaor, B. Bécsy, C. Chapman, M. Charisi, S. Chatterjee, T. Cohen, J. M. Cordes, N. J. Cornish, F. Crawford, H. T. Cromartie, K. Crowter, M. E. Decesar, P. B. Demorest, T. Dolch, B. Drachler, E. C. Ferrara, W. Fiore, E. Fonseca, G. E. Freedman, N. Garver-Daniels, P. A. Gentile, J. Glaser, D. C. Good, K. Gültekin, J. S. Hazboun, R. J. Jennings, C. Jessup, A. D. Johnson, M. L. Jones, A. R. Kaiser, D. L. Kaplan, L. Z. Kelley, M. Kerr, J. S. Key, A. Kuske, N. Laal, M. T. Lam, W. G. Lamb, T. J. W. Lazio, N. Lewandowska, Y. Lin, T. Liu, D. R. Lorimer, J. Luo, R. S. Lynch, C.-P. Ma, D. R. Madison, K. Maraccini, A. McEwen, J. W. McKee, M. A. McLaughlin, N. McMann, B. W. Meyers, C. M. F. Mingarelli, A. Mitridate, C. Ng, D. J. Nice, S. K. Ocker, K. D. Olum, E. Panciu, T. T. Pennucci, B. B. P. Perera, N. S. Pol, H. A. Radovan, S. M. Ransom, P. S. Ray, J. D. Romano, L. Salo, S. C. Sardesai, C. Schmiedekamp, A. Schmiedekamp, K. Schmitz, B. J. Shapiro-Albert, X. Siemens, J. Simon, M. S. Siwek, I. H. Stairs, D. R. Stinebring, K. Stovall, A. Susobhanan, J. K. Swiggum, S. R. Taylor, J. E. Turner, C. Unal, M. Vallisneri, S. J. Vigeland, H. M. Wahl, Q. Wang, C. A. Witt, O. Young, and Nanograv Collaboration, The NANOGrav 15 yr Data Set: Observations and Timing of 68 Millisecond Pulsars, *ApJL* **951**, L9 (2023), arXiv:2306.16217 [astro-ph.HE].
- [53] T. Damour and J. H. Taylor, Strong-field tests of relativistic gravity and binary pulsars, *Phys. Rev. D* **45**, 1840 (1992).
- [54] R. J. Jennings, D. L. Kaplan, S. Chatterjee, J. M. Cordes, and A. T. Deller, Binary Pulsar Distances and Velocities from Gaia Data Release 2, *Astrophys. J.* **864**, 26 (2018), arXiv:1806.06076 [astro-ph.SR].
- [55] J. C. A. Miller-Jones, A. T. Deller, R. M. Shannon, R. Dodson, J. Moldón, M. Ribó, G. Dubus, S. Johnston, J. M. Paredes, S. M. Ransom, and J. A. Tomsick, The geometric distance and binary orbit of PSR B1259-63, *MNRAS* **479**, 4849 (2018), arXiv:1804.08402 [astro-ph.HE].
- [56] H. Ding, A. T. Deller, E. Fonseca, I. H. Stairs, B. Stappers, and A. Lyne, The Orbital-decay Test of General Relativity to the 2% Level with 6 yr VLBA Astrometry of the Double Neutron Star PSR J1537+1155, *ApJL* **921**, L19 (2021), arXiv:2110.10590 [astro-ph.HE].
- [57] A. T. Deller, J. M. Weisberg, D. J. Nice, and S. Chatterjee, A VLBI Distance and Transverse Velocity for PSR B1913+16, *Astrophys. J.* **862**, 139 (2018), arXiv:1806.10265 [astro-ph.SR].
- [58] J. Antoniadis, Gaia pulsars and where to find them, *MNRAS* **501**, 1116 (2021), arXiv:2011.08075 [astro-ph.HE].
- [59] A. Moran, C. M. F. Mingarelli, M. Bedell, and D. Good, Further Improving Distances to Binary Millisecond Pulsars with Gaia EDR3, arXiv e-prints , arXiv:2210.10816 (2022), arXiv:2210.10816 [astro-ph.IM].
- [60] B. B. P. Perera, M. E. DeCesar, P. B. Demorest, M. Kerr, L. Lentati, D. J. Nice, S. Osłowski, S. M. Ransom, M. J. Keith, Z. Arzoumanian, M. Bailes, P. T. Baker, C. G. Bassa, N. D. R. Bhat, A. Brazier, M. Burgay, S. Burke-Spolaor, R. N. Caballero, D. J. Champion, S. Chatterjee, S. Chen, I. Cognard, J. M. Cordes, K. Crowter, S. Dai, G. Desvignes, T. Dolch, R. D. Ferdman, E. C. Ferrara, and E. Fonseca, The International Pulsar Timing Array: second data release, *MNRAS* **490**, 4666 (2019), arXiv:1909.04534 [astro-ph.HE].
- [61] K. Stovall, R. S. Lynch, S. M. Ransom, A. M. Archibald, S. Banaszak, C. M. Biwer, J. Boyles, L. P. Dartez, D. Day, A. J. Ford, J. Flanagan, A. Garcia, J. W. T. Hessels, J. Hinojosa, F. A. Jenet, D. L. Kaplan, C. Karakoc-Argaman, V. M. Kaspi, V. I. Kondratiev, S. Leake, D. R. Lorimer, G. Lunsford, J. G. Martinez, A. Mata, M. A. McLaughlin, M. S. E. Roberts, M. D. Rohr, X. Siemens, I. H. Stairs, J. van Leeuwen, A. N. Walker, and B. L. Wells, The Green Bank Northern Celestial Cap Pulsar Survey. I. Survey Description, Data Analysis, and Initial Results, *Astrophys. J.* **791**, 67 (2014), arXiv:1406.5214 [astro-ph.HE].
- [62] A. T. Deller, M. Bailes, and S. J. Tingay, Implications of a VLBI Distance to the Double Pulsar J0737-3039A/B,

- Science **323**, 1327 (2009), arXiv:0902.0996 [astro-ph.SR].
- [63] E. Fonseca, H. T. Cromartie, T. T. Pennucci, P. S. Ray, A. Y. Kirichenko, S. M. Ransom, P. B. Demorest, I. H. Stairs, Z. Arzoumanian, L. Guillemot, A. Parthasarathy, M. Kerr, I. Cognard, P. T. Baker, H. Blumer, P. R. Brook, M. DeCesar, T. Dolch, F. A. Dong, E. C. Ferrara, W. Fiore, N. Garver-Daniels, D. C. Good, R. Jennings, M. L. Jones, V. M. Kaspi, M. T. Lam, D. R. Lorimer, J. Luo, A. McEwen, J. W. McKee, M. A. McLaughlin, N. McMann, B. W. Meyers, A. Naidu, C. Ng, D. J. Nice, N. Pol, H. A. Radovan, B. Shapiro-Albert, C. M. Tan, S. P. Tendulkar, J. K. Swiggum, H. M. Wahl, and W. W. Zhu, Refined Mass and Geometric Measurements of the High-mass PSR J0740+6620, ApJL **915**, L12 (2021), arXiv:2104.00880 [astro-ph.HE].
- [64] D. J. Reardon, G. Hobbs, W. Coles, Y. Levin, M. J. Keith, M. Bailes, N. D. R. Bhat, S. Burke-Spolaor, S. Dai, M. Kerr, P. D. Lasky, R. N. Manchester, S. Osłowski, V. Ravi, R. M. Shannon, W. van Straten, L. Toomey, J. Wang, L. Wen, X. P. You, and X. J. Zhu, Timing analysis for 20 millisecond pulsars in the Parkes Pulsar Timing Array, MNRAS **455**, 1751 (2016), arXiv:1510.04434 [astro-ph.HE].
- [65] P. C. C. Freire, N. Wex, G. Esposito-Farèse, J. P. W. Verbiest, M. Bailes, B. A. Jacoby, M. Kramer, I. H. Stairs, J. Antoniadis, and G. H. Janssen, The relativistic pulsar-white dwarf binary PSR J1738+0333 - II. The most stringent test of scalar-tensor gravity, MNRAS **423**, 3328 (2012), arXiv:1205.1450 [astro-ph.GA].
- [66] R. D. Ferdman, I. H. Stairs, M. Kramer, G. H. Janssen, C. G. Bassa, B. W. Stappers, P. B. Demorest, I. Cognard, G. Desvignes, G. Theureau, M. Burgay, A. G. Lyne, R. N. Manchester, and A. Possenti, PSR J1756-2251: a pulsar with a low-mass neutron star companion, MNRAS **443**, 2183 (2014), arXiv:1406.5507 [astro-ph.SR].
- [67] A. T. Deller, J. Boyles, D. R. Lorimer, V. M. Kaspi, M. A. McLaughlin, S. Ransom, I. H. Stairs, and K. Stovall, VLBI Astrometry of PSR J2222-0137: A Pulsar Distance Measured to 0.4% Accuracy, Astrophys. J. **770**, 145 (2013), arXiv:1305.4865 [astro-ph.SR].
- [68] K. Stovall, P. C. C. Freire, J. Antoniadis, M. Bagchi, J. S. Deneva, N. Garver-Daniels, J. G. Martinez, M. A. McLaughlin, Z. Arzoumanian, H. Blumer, P. R. Brook, H. T. Cromartie, P. B. Demorest, M. E. DeCesar, T. Dolch, J. A. Ellis, R. D. Ferdman, E. C. Ferrara, E. Fonseca, P. A. Gentile, M. L. Jones, M. T. Lam, D. R. Lorimer, R. S. Lynch, C. Ng, D. J. Nice, T. T. Pennucci, S. M. Ransom, R. Spiewak, I. H. Stairs, J. K. Swiggum, S. J. Vigeland, and W. W. Zhu, PSR J2234+0611: A New Laboratory for Stellar Evolution, Astrophys. J. **870**, 74 (2019), arXiv:1809.05064 [astro-ph.HE].
- [69] R. W. Romani and M. S. Shaw, The Orbit and Companion of Probable γ -Ray Pulsar J2339-0533, ApJL **743**, L26 (2011), arXiv:1111.3074 [astro-ph.HE].

Appendix A: Catalog summary

In Tab. III of this supplement we present the data for each pulsar in our catalog. This includes position and orbital measurements as well as intermediate calculations of \dot{P}_b^{Kin} and final calculations of a_{Gal} . Complete data are available in an appended .xls file.

We also present maps of the pulsars and acceleration data in Figs. 4, 5, and 6. In addition to sky position, Fig. 4 shows the portion of pulsars in our catalog which are monitored by the International Pulsar Timing Array (IPTA) or are millisecond pulsars (MSPs). The pulsars are all within 5 kpc of Earth (see Fig. 4, and Fig. 7). Furthermore, all but two of the pulsars are in the galactic disk, Fig. 6. This distribution is consistent with the assumptions of the radial gradient expansion we use to model galactic acceleration (Eq. 5 of the main text).

TABLE III. Data for each pulsar: the galactocentric coordinates x, y, z , observed binary period P_b and its first time derivative \dot{P}_b^{Obs} , predicted binary period derivative \dot{P}_b^{Kin} from kinematic effects, our inferred line-of-sight acceleration a_{Gal} , and the reference used for the distance measurement. A star '*' next to $\log_{10}|\dot{P}_b^{\text{Obs}}|$ values indicates that \dot{P}_b^{Obs} is negative. A dagger '†' next to a pulsar's name indicates that a_{Gal} is calculated with the approximation $e \approx 0$ due to a lack of an eccentricity determination, while a double dagger '‡' next to the pulsar's name indicates the approximation $M_p = 1.57 \pm 0.35 M_\odot$ was used.

Pulsar	x [pc]	y [pc]	z [pc]	P_b [10^4 s]	$\log_{10} \dot{P}_b^{\text{Obs}} $	\dot{P}_b^{Kin} [10^{-14}]	a_{Gal} [$10^{-10} \text{ m s}^{-2}$]	Ref.
B1259-63	6661.5	-2150.5	-27.9	10 700.00	-7.85 (-8.15)	3360 \pm 450	391 \pm 196	[55]
B1534+12	7532.5	212.1	721.6	3.64	-12.9 * (-15.5)	5.34 \pm 0.37	0.093 \pm 0.313	[56]
B1913+16	5486.2	3137.1	165.9	2.79	-16.6 * (-15.0)	0.0145 \pm 0.0086	-4.74 \pm 0.15	[57]
J0348+0432	10 116.9	-116.1	-1464.7	0.89	-12.6 * (-13.3)	0.153 \pm 0.076	-5.6 \pm 18.2	[58]
J0437-4715	8155.6	-111.9	-84.1	49.60	-11.4 (-14.2)	377.3 \pm 0.1	-0.256 \pm 0.050	[59]
J0613-0200	9067.1	-554.5	-156.3	10.40	-13.7 (-14.1)	3.10 \pm 0.14	-0.140 \pm 0.532	[60]
J0636+5129	8313.0	55.2	88.4	0.58	-21.5 (-22.9)	0.00387 \pm 0.00052	27.3 \pm 21.9	[61]
J0737-3039A/B	8602.4	-1041.0	-68.3	0.88	-11.9 * (-13.8)	0.0472 \pm 0.0157	-1.6 \pm 11.3	[62]
J0740+6620	8984.1	504.0	591.0	41.20	-11.9 (-12.7)	122 \pm 17	0.17 \pm 1.91	[63]
J0751+1807	9325.5	-504.7	527.6	2.27	-13.5 * (-14.6)	1.45 \pm 0.37	-0.80 \pm 2.90	[60]
J1012+5307†	8617.9	177.7	671.2	5.22	-13.2 (-14.0)	7.02 \pm 0.12	-0.249 \pm 0.685	[59]
J1017-7156	7620.6	-1270.9	-284.8	56.30	-12.4 (-12.7)	19.7 \pm 25.3	1.09 \pm 1.72	[64]
J1022+1001	8400.2	-355.3	581.9	67.40	-12.7 (-13.2)	30.0 \pm 0.6	-0.406 \pm 0.305	[60]
J1125-6014	7547.9	-1385.6	42.7	75.60	-12.2 (-13.0)	80.8 \pm 43.1	-0.43 \pm 1.75	[64]
J1600-3053	6395.9	-491.6	546.0	124.00	-12.3 (-13.0)	27.8 \pm 3.6	0.536 \pm 0.257	[64]
J1603-7202	7749.3	-352.4	-112.8	5.45	-12.7 (-13.4)	4.2 \pm 14.3	0.815 \pm 0.818	[64]
J1614-2230	7479.1	-83.0	257.3	75.10	-11.8 (-12.9)	132 \pm 10	0.977 \pm 0.653	[60]
J1713+0747	7168.9	522.2	529.7	586.00	-12.7 (-13.0)	67.7 \pm 1.7	-0.244 \pm 0.052	[60]
J1738+0333	6881.4	651.3	465.6	3.07	-13.8 * (-14.5)	0.824 \pm 0.056	0.21 \pm 1.03	[65]
J1741+1351	6799.8	1027.4	681.2	5.88	-11.9 (-12.4)	3.49 \pm 0.78	67.5 \pm 18.8	[51]
J1756-2251	7178.2	107.5	34.1	2.76	-12.6 * (-14.3)	0.037 \pm 0.617	-1.36 \pm 1.15	[66]
J1909-3744‡	7048.9	-5.0	-364.3	13.20	-12.3 (-15.2)	50.2 \pm 0.4	0.234 \pm 0.101	[60]
J2043+1711	7396.6	1361.5	-403.6	0.53	-13.0 (-13.9)	0.311 \pm 0.039	323 \pm 194	[52]
J2129-5721	7720.0	-162.8	-393.8	57.20	-11.8 (-13.0)	14.9 \pm 9.9	7.14 \pm 0.70	[60]
J2145-0750	7813.8	340.8	-395.5	59.10	-12.9 (-13.7)	15.4 \pm 0.1	-0.120 \pm 0.102	[60]
J2222-0137	8035.6	163.6	-171.7	21.10	-12.6 (-14.1)	27.8 \pm 0.2	-0.281 \pm 0.125	[67]
J2234+0611	7920.4	664.3	-627.7	27.60	-11.5 (-11.6)	468 \pm 20	-1.72 \pm 2.72	[68]
J2339-0533	8025.1	657.9	-1256.5	1.67	-19.7 * (-21.7)	0.719 \pm 0.167	4.26 \pm 1.96	[69]

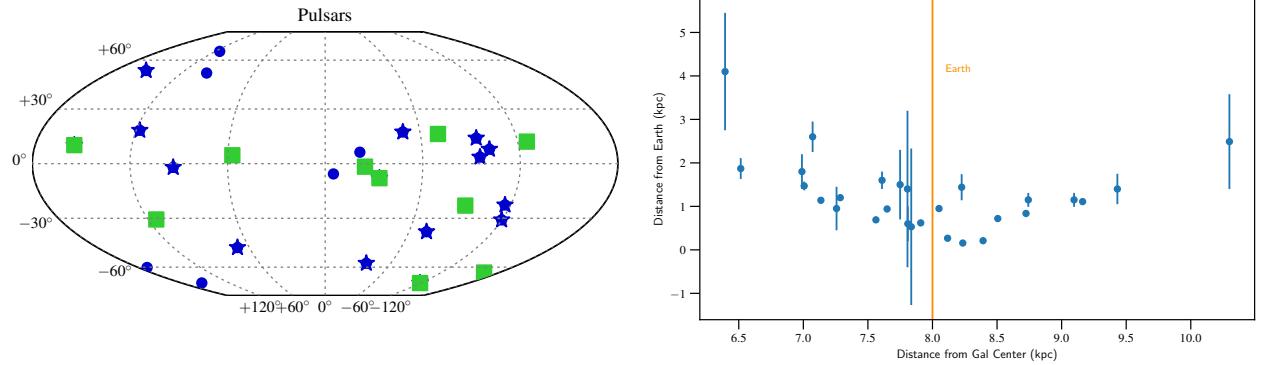


FIG. 4. Left: Locations of the 228 pulsars included in this data release. IPTA and other MSPs are shown in blue, with star and circle markers respectively. Green squares are not MSPs, however they do have measured binary orbital period derivatives. Right: Distances to the 28 pulsars in this data release.

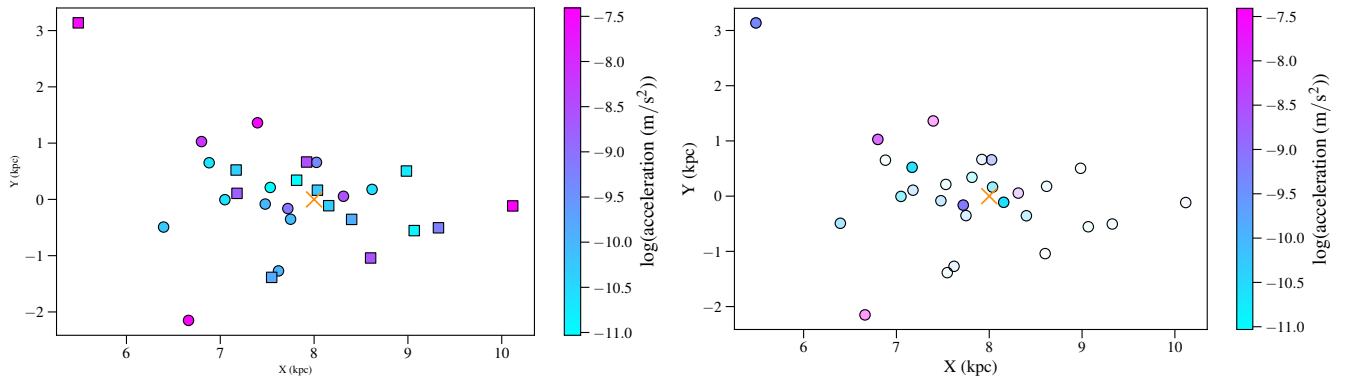


FIG. 5. The acceleration data mapped as a function of position in galactocentric coordinates, from a top-down view of the Milky Way. In both panels, the orange “X” is the Earth. The left panel shows the log of the absolute value of the accelerations as a function of position. Square points indicate negative accelerations, while circular ones are positive. The right panel shows the log of the acceleration data with relative uncertainty indicated by opacity; more faint points have higher values of uncertainty relative to calculated acceleration.

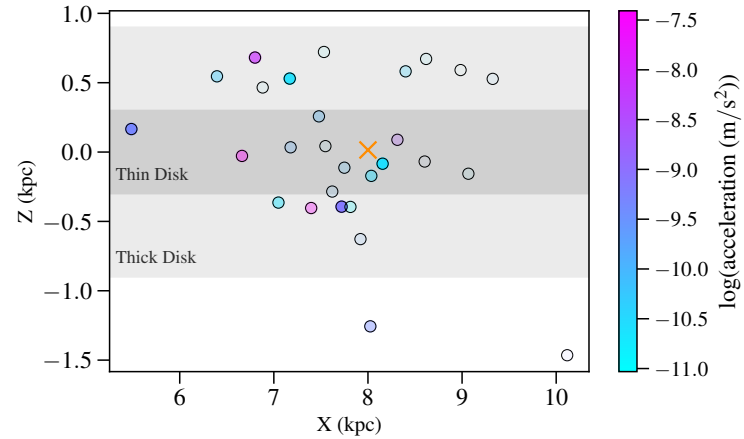


FIG. 6. Acceleration data mapped over an edge on view of the Milky Way in galactocentric coordinates, where the orange X is the Earth. As in Fig. 5, more faded points represent acceleration values with higher relative uncertainties. All but two of the pulsars are within the galactic disk, and 12 of the 28 are in the thin disk.

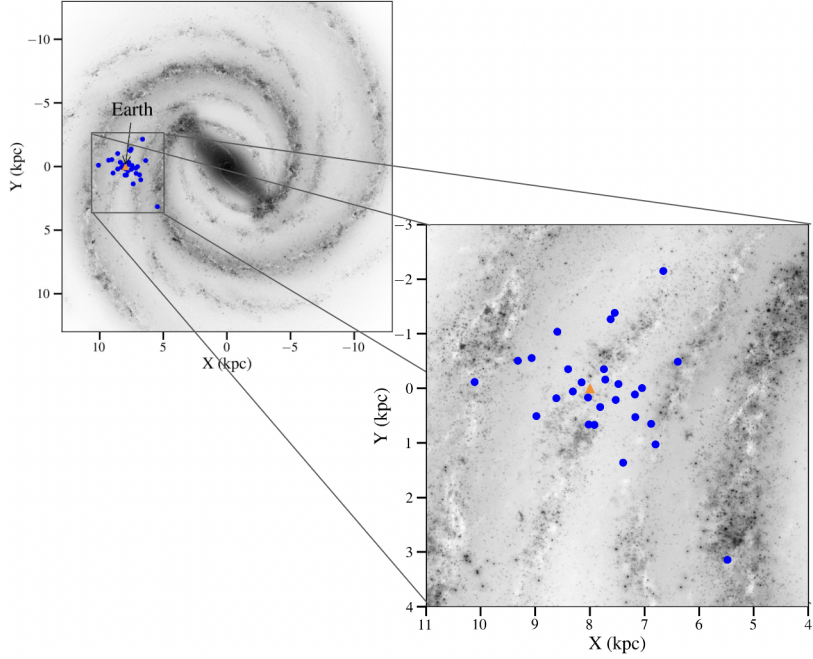


FIG. 7. A “top-down” 2D look at the distribution of the selected binary pulsars in the Galaxy in galactocentric coordinates. While all of the pulsars are clustered around Earth (shown in orange) right now, we are hopeful that with new *Gaia* data releases we will be able to add pulsars further from the Earth as we find more parallax measurements.